Solid-State Electronics 104 (2015) 47–52

Contents lists available at ScienceDirect

Solid-State Electronics

journal homepage: www.elsevier.com/locate/sse

Angle dependent conductivity in graphene FET transistors

C.H. Fuentevilla [a], J.D. Lejarreta [a], C. Cobaleda [b], E. Diez [b,*]

[a] Departamento de Física Aplicada, Universidad de Salamanca, E-37008 Salamanca, Spain
[b] Departamento de Física Fundamental, Universidad de Salamanca, E-37008 Salamanca, Spain

ARTICLE INFO

Article history:
Received 21 February 2014
Received in revised form 6 October 2014
Accepted 11 November 2014
Available online 1 December 2014

The review of this paper was arranged by Dr. Y. Kuk

Keywords:
Graphene
Field effect transistors
Disorder
Electronic transport

ABSTRACT

In this work we analyze a model of conductance across a field effect transistor built of monolayer graphene. We show how a top gate voltage non-perpendicular to the source-drain direction creates an effective gap in pristine graphene devices. We have studied several scenarios in order to model the presence of inhomogeneities in the graphene and its influence in the creation of an effective gap showing that it is a robust effect. Moreover, although the gap appears for any angle of the top-gate, tuning the FET parameters we achieve noticeable on–off ratios overcoming one of the main difficulties of graphene transistors.

1. Introduction

Monolayer graphene is a one – atom thick carbon layer in a hexagonal honeycomb lattice. From the lattice properties, it is possible to deduce the band structure, and hence the energy spectrum. In graphene, charge carriers are described by the Dirac equation instead of Schrödinger's, as is the case of traditional semiconductors. This is a direct consequence of the fact that graphene has two equivalent triangular sublattices, A and B [1]. Therefore, the dispersion relationship is linear [2] and hence the carriers in graphene have the same dispersion relationship as massless particles with velocity $v_F \sim c/300$.

According to previous studies, graphene might be an ideal material for electronic devices [3–5] due to several of its properties, such as its high mobility (up to 15,000 cm^2/Vs [6]), the large scattering length [7] and also because graphene can stand a current density that is six orders of magnitude greater than copper [8]. The conductance of PN junctions in graphene has been studied previously [9] and different configurations of NNN, NPN, PPP and PNP junctions have also been studied [10]. Experimental measurements have been carried out in order to study the conducting properties of PNP structures [11] obtained by the deposition of a top gate separated from the graphene by an air gap. Quantum oscillations of the conductance in graphene have been studied both theoretically [12] and experimentally [13,14].

Because of its electrical properties, graphene is an interesting potential material to develop nanodevices for use in technological applications, such as field effect transistors (FET). In this work we have modeled a FET based on graphene and analyzed its electrical transport capabilities based on an exact analytical solution to the Dirac equation found previously [15]. Finally, we study the different behavior of the conductance shown by a FET, considering that the current does not flow perpendicularly to the top gate. Let us stress our model is devoted to graphene FET transistors with high mobility, when electronic transport is dominated by ballistic carriers. On the opposite limit, when transport is dominated by scattering, *i.e.*, CVD graphene samples, a drift–diffusion model should be considered [16,17].

2. Model

Fig. 1 shows a scheme of the device under consideration: a rectangular single layer of graphene (blue), with two gold contacts for the source and drain. The device also has a back gate and a top gate which is placed on the dielectric layer (SiO_2, PMMA resist or RX resist, for example). The back gate controls the charge carrier density of the sample and the top gate modulates the current that flows through the device from source to drain, passing through a square potential barrier. We shall assume that the sample is big enough not to be considered as a strip, and therefore that there will be no edge effects. Furthermore, at temperatures close to 0 K, the charge carrier density n is proportional to the Fermi energy

* Corresponding author. Tel.: +34 923 29 44 35; fax: +34 923 29 45 84.
E-mail address: enrisa@usal.es (E. Diez).

http://dx.doi.org/10.1016/j.sse.2014.11.007
0038-1101/

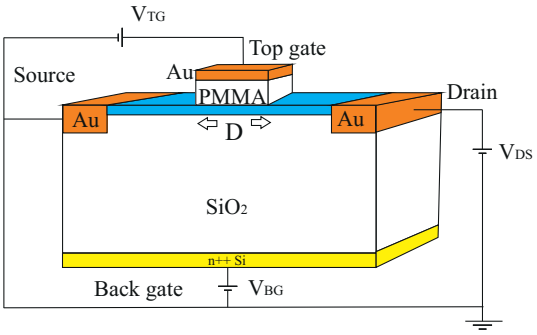

Fig. 1. Scheme of the device studied in this paper. A sheet of graphene is in blue. (For interpretation of the references to color in this figure legend, the reader is referred to the web version of this article.)

squared [18] ($n \propto E_F^2$) and will show a linear dependence on the back gate voltage ($n \propto V_{BG}$) [10].

In order to explain the behavior of such a device by characterizing its conductance in several regimes, we have to start – bearing in mind that "conductance is transmission" [19] – by considering the transmission of the electrons across the device. Here, the electrons of the graphene are transmitted as massless ultrarelativistic Dirac particles subjected to a potential barrier governed by the potential gates. This problem has already been considered and we have an analytical transmission coefficient [15,20] that we shall use here. The transmission coefficient across the barrier (Fig. 2) is

$$T(E,V_0,D,\phi)=\left(1+V_0^2\tan^2\phi\frac{\sin^2\left(\frac{D}{\hbar v_F}\sqrt{(E-V_0)^2-E^2\sin^2\phi}\right)}{(E-V_0)^2-E^2\sin^2\phi}\right)^{-1} \quad (1)$$

As can be seen, the transmission coefficient depends upon the energy of the charge carrier E, the angle of incidence ϕ and the parameters of the barrier potential V_0 and D, whereas it does not depend upon the dimensions of the graphene sheet W and L. Also, the transmission coefficient is symmetric with respect to the angle of incidence ϕ. According to this expression, in the case of normal incidence the transmission coefficient is unity, with independence of any other parameters. This is the case of the Klein paradox for Dirac particles [21–23].

The analytical expression obtained for the transmission coefficient can now be used in order to calculate the conductance across a potential barrier. At ultra – low temperatures (at zero temperature) the conductance of this FET is [15]

$$G_{eff}=\frac{2}{\hbar v_F \pi}|E_F|\int_{-\pi/2}^{+\pi/2}T(E_F,V_0,D,\phi)\cos\phi\, d\phi \quad (2)$$

Note that if we express the lengths in nm and the energies in meV, we have $\hbar v_F = 658.2$ meV nm and the effective conductance is given in units of e^2/h.

The conductance will depend on the potential applied by the top gate (through the transmission coefficient), the potential applied by the back gate (through E_F) and the width of the graphene sheet, but not upon its length.

Furthermore, we observe in (Eq. (2)) that the maximun value of the effective conductance is at $T(E_F,V_0,D,\phi)=1$, and therefore

$$G_{eff,max}=\frac{4}{\hbar v_F \pi}|E_F| \quad (3)$$

By introducing the expression in Eq. (1) into Eq. (2) we obtain the effective conductance for one square barrier potential in graphene:

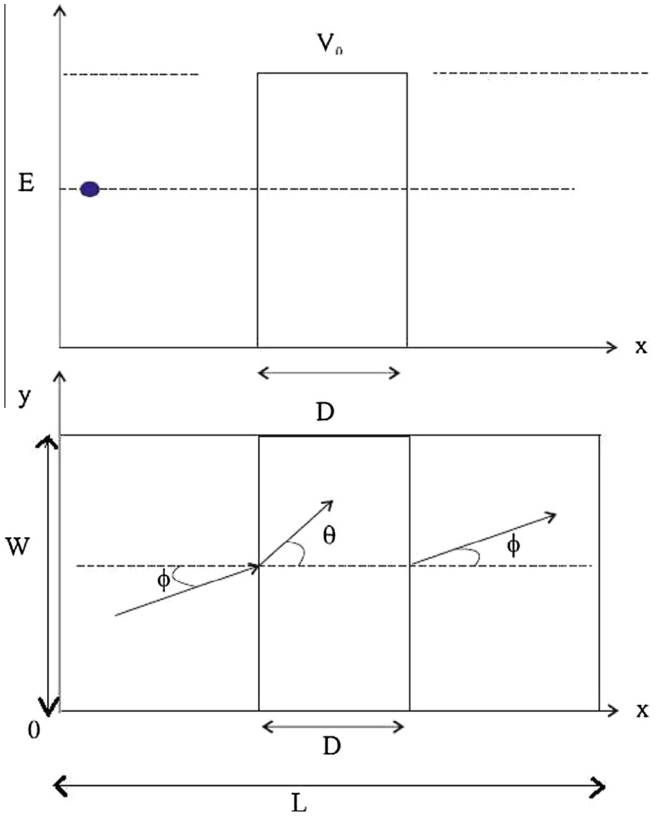

Fig. 2. Top panel: carrier energy and barrier potential dependence with the position in the sample. Bottom panel: scheme of the graphene layer and angles of incidence at the barrier potential.

$$G_{eff}(E_F,V_0,D)=\frac{2|E_F|}{\hbar v_F \pi}\int_{-\pi/2}^{+\pi/2}\left(1+V_0^2\tan^2\phi\frac{\sin^2\left(\frac{D}{\hbar v_F}\sqrt{(E_F-V_0)^2-E_F^2\sin^2\phi}\right)}{(E_F-V_0)^2-E_F^2\sin^2\phi}\right)^{-1}\cos\phi\, d\phi \quad (4)$$

As seen, the effective conductance of a graphene-based FET depends on the Fermi energy and the properties of the potential barrier created by the top gate (height V_0 and width D).

Fig. 3 shows conductance versus Fermi energy. It is seen that the curve of the effective conductance has a local maximum when $E_F = 0.5V_0$. At this point, the sign of the quantity $(E_F-V_0)^2 - E_F^2\sin^2\phi$ is changed from positive to negative. Therefore, in (Eq. (4)) the sine of this quantity will become a hyperbolic sine, and conductance will become smaller. Thus, the resistance will increase. This situation will persist until a local minimum is reached, at $E_F \simeq V_0$. When E_F is greater than V_0, since the transmission coefficient tends to unity, the effective conductance grows proportionally to the Fermi energy, similarly to (Eq. (3)). We observe oscillations of the conductance at Fermi energies that satisfy the condition $E_F < V_0$. For $E_F < 0.5V_0$, there are several oscillations, whereas for values of the Fermi energy such that $0.5V_0 < E_F < V_0$ there is only one oscillation. If $E_F \gg V_0$, the conductance does not depend on the value of the barrier width and varies linearly with the Fermi energy.

As may be seen in Fig. 4, when V_0 increases, the effective conductance decreases linearly and takes the same value independently of the value of the width, for V_0, satisfying $V_0 < E_F$. When V_0 takes the value of the Fermi energy, there is a local minimum whose value depends on the width of the barrier D. For $V_0 > E_F$, the conductance increases and exhibits oscillations which become larger as the width of the barrier decreases. These oscillations appear only for values of V_0 that satisfy $V_0 > E_F$.

The dependence of the effective conductance upon the width D of the barrier is shown in Fig. 5. The conductance decreases until it

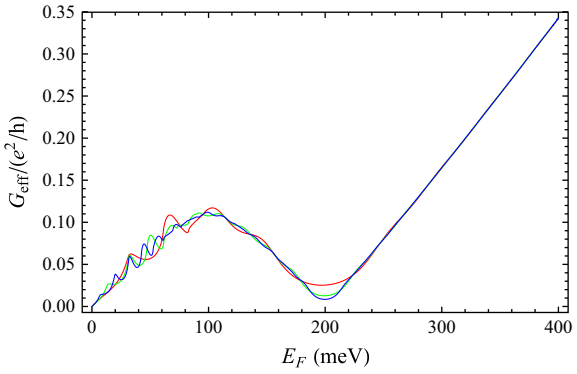

Fig. 3. Effective conductance versus Fermi energy at barrier height $V_0 = 200$ meV and barrier width D 50 (red), 100 (green) and 150 (blue) nm. Conductance has a local maximum at $E_F = 0.5V_0$, a local minimum at $E_F = V_0$ and increases linearly with $E_F \geqslant V_0$. (For interpretation of the references to color in this figure legend, the reader is referred to the web version of this article.)

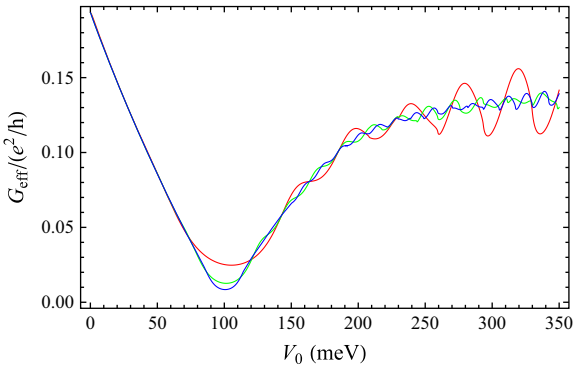

Fig. 4. Conductance versus height of the barrier at Fermi energies $E_F = 100$ meV and D 50 (red), 100 (green) and 150 (blue) nm. The three curves take the same values for $E_F > V_0$, and show a minimum for $E_F = V_0$. The amplitude of the oscillations depends on the value of the width of the barrier D. (For interpretation of the references to color in this figure legend, the reader is referred to the web version of this article.)

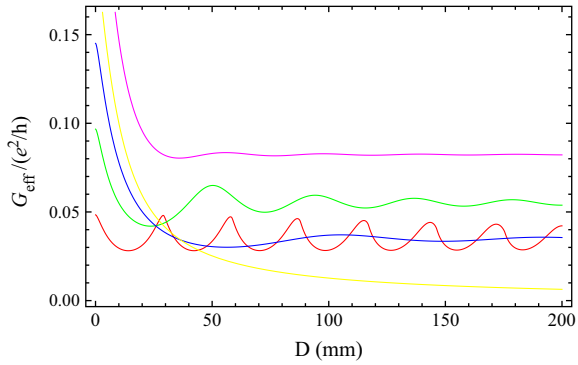

Fig. 5. Conductance versus barrier width when assuming a barrier height $V_0 = 100$ meV and Fermi energies $E_F = 25$ (red), 50 (green), 75 (blue), 100 (yellow) and 150 (purple) meV in order to perform the calculations. (For interpretation of the references to color in this figure legend, the reader is referred to the web version of this article.)

becomes stabilised in the vicinity of a constant value. It is also observed that the oscillations tend to be lower as the Fermi energy increases.

3. Weighted effective conductance

Up to now we have considered that the carriers scatter through the barrier with the same probability for each angle of incidence. Other scenarios should also be considered in which, due to the inhomogeneities of the material or the design of the device, the carriers flow around a certain direction. Thus, the angle of incidence will, in general, be different from 0° and will obey a certain probability distribution function $P(\phi)$ centered around an angle ϕ_0. This probability distribution function must satisfy the condition

$$\int_{-\pi/2}^{+\pi/2} P(\phi)d\phi = \pi \tag{5}$$

Below, we shall consider different probabilities of distribution and we shall study their effect on the effective conductance.

3.1. Gaussian distribution

We now consider the case of a Gaussian function for the probability distribution of the incidence angle. This assumption represents the idea that transport is of ballistic nature and that there are few inhomogeneities that cause scattering processes within the sample and deviate carriers from their ballistic trajectory, leading them to impact on the barrier potential with diverse incidence angles. Since not all the carriers will undergo the same scattering process, we can assume that the majority of carriers will impact on the barrier potential with a similar angle, ϕ_0, and that there will be more carriers impacting on the barrier potential with an angle of incidence ϕ_0 than carriers impacting on the barrier with an angle of incidence that differs substantially from ϕ_0. Thus, we assume that the angles of incidence of the carriers will obey a probability distribution function of the form $P(\phi) = c\exp\left(-\frac{(\phi-\phi_0)^2}{2a^2}\right)$.

The parameter a of the Gaussian functions makes the distinction between a homogeneous sample (a narrow Gaussian bell) and a sample with many of inhomogeneities (a wide distribution). A narrow Gaussian function represents the case in which almost all the carriers scatter with the barrier at the same angle of incidence. This will happen when the sample is homogeneous and the carriers do not scatter with the sample inhomogeneities, and therefore the transport will be ballistic and almost all the carriers will move through the sample with a similar direction. Obviously, a wide Gaussian function represents the opposite case.

We start the analysis by considering the centered angle of our Gaussian distribution being: $\phi_0 = 0°$. Obviously, the parameters a and c are not independent since they must hold the normalization condition $ac\sqrt{2\pi}Erf\left(\frac{\pi}{2\sqrt{2}a}\right) = \pi$. As we can see, as c becomes smaller, a becomes greater.

The conductance is given by:

$$G_g(E_F, V_0, D) = \frac{2c}{\hbar v_F \pi}|E_F| \int_{-\pi/2}^{+\pi/2} T(E_F, V_0, D, \phi) \times \cos\phi \exp\left(-\frac{\phi^2}{2a^2}\right)d\phi \tag{6}$$

As in the previous case, the effective conductance depends on E_F, V_0 and D but it shows a different behavior, as shown in Figs. 6 and 7.

Next, we study the behavior of the conductance when the Fermi energy is changed while the other variables remain at fixed values (see Fig. 6). The conductance oscillates while it increases until a local maximum is reached. The value and position of this maximum now depend on the parameters of the Gaussian function used. Once the maximum is reached, the conductance decreases until it reaches a local minimum when $E_F \sim V_0$. Once the minimum is surpassed, the conductance increases monotonically (see Fig. 8).

As shown in Fig. 7, when using V_0 as the driving parameter and the other parameters remain fixed at constant values, we can see that the effective conductance decreases until it reaches a

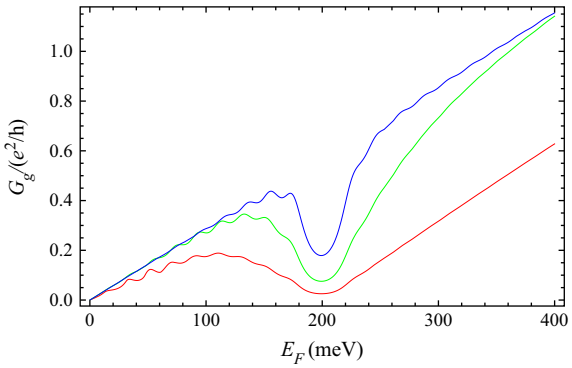

Fig. 6. Effective conductance versus the Fermi energy when the distribution function of the angle of incidence is a Gaussian function centered around $\phi_0 = 0^\circ$ assuming different widths of the Gaussian: 0.64 (red), 0.21 (green) and 0.08 (blue). The height of the barrier is $V_0 = 200$ meV and its width is $D = 100$ nm. (For interpretation of the references to color in this figure legend, the reader is referred to the web version of this article.)

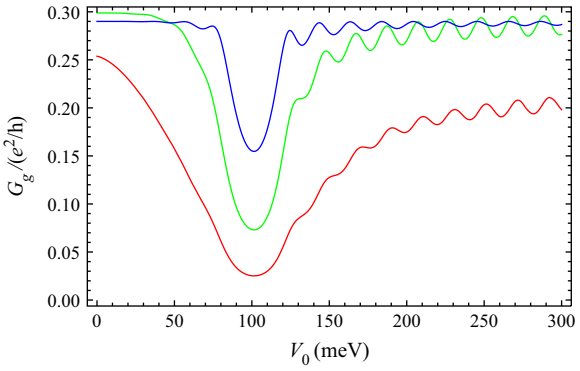

Fig. 7. Conductance versus the height of the barrier V_0 asuming a Gaussian probability distribution function centered around $\phi_0 = 0^\circ$. The width of the Gaussian distribution is $a = 0.64$ (red), $a = 0.21$ (green) and $a = 0.08$ (blue). The Fermi energy of the system is assumed to be $E_F = 100$ meV and the width of the barrier is $D = 100$ nm. (For interpretation of the references to color in this figure legend, the reader is referred to the web version of this article.)

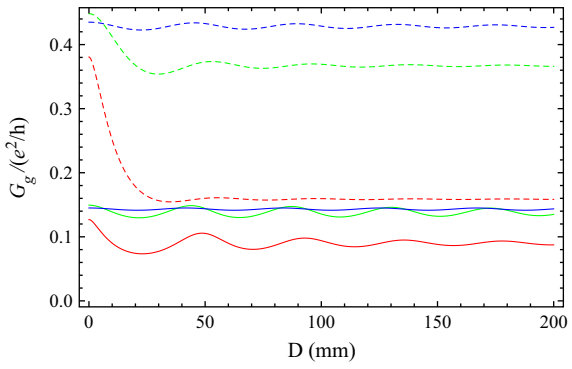

Fig. 8. Conductance versus barrier width using a Gaussian distribution of probability centered around $\phi_0 = 0^\circ$. The width of the Gaussian is assumed to be $a = 0.64$ (red), $a = 0.21$ (green) and $a = 0.08$ (blue). The Fermi energy is $E_F = 50$ meV (line) and $E_F = 150$ meV (dashed line). Also, the barrier height is $V_0 = 100$ meV. (For interpretation of the references to color in this figure legend, the reader is referred to the web version of this article.)

minimum around $E_F \sim V_0$. It is also observed that the narrower the Gaussian function (which is equivalent to a less disordered distribution), the more pronounced the variation in the conductance. Once E_F is greater than V_0 we observe aperiodic oscillations of the conductance, whose frequency tends to the value $\omega = 2D/\hbar v_F$.

We now consider the case in which the Gaussian distribution is not centered around $\phi_0 = 0^\circ$. This might be done by tilting the orientation of the top gate in a graphene – based device as shown in for example [24]. In this case, the normalization condition is given by the expression $ac\sqrt{\frac{\pi}{2}}\left(Erf\left(\frac{-2\phi_0+\pi}{2\sqrt{2}\cdot a}\right) + Erf\left(\frac{2\phi_0+\pi}{2\sqrt{2}\cdot a}\right)\right) = \pi$.

As we see in Figs. 9 and 10, the results are similar to those obtained in the previous case, but the minima observed previously are wider. In fact, as a becomes closer to zero these minima become wider (see Fig. 11).

3.2. Delta distribution

We now consider the extreme scenario in which the Gaussian function is so narrow that it can be represented by a Delta function $\delta(\phi - \phi_0)$. This is the case in which the material is ideal and all the carriers scatter through the barrier with the same angle of incidence, ϕ_0.

In this case, the conductance is given by:

$$G_{d,\phi_0}(E_F, V_0, D) = \frac{2|E_F|}{\hbar v_F} T(E_F, V_0, D, \phi_0)\cos\phi_0 \tag{7}$$

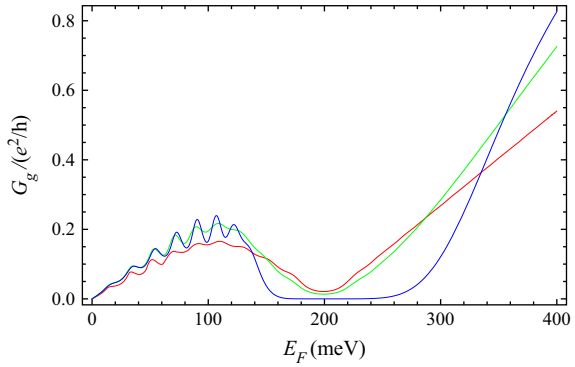

Fig. 9. Conductance versus the Fermi energy considering that the distribution is a Gaussian function centered around $\phi_0 = 22.5^\circ$ using different widths for the Gaussian function: $a = 0.65$ (red), $a = 0.21$ (green), $a = 0.08$ (blue). The height of the barrier is $V_0 = 200$ meV and its width $D = 100$ nm. (For interpretation of the references to color in this figure legend, the reader is referred to the web version of this article.)

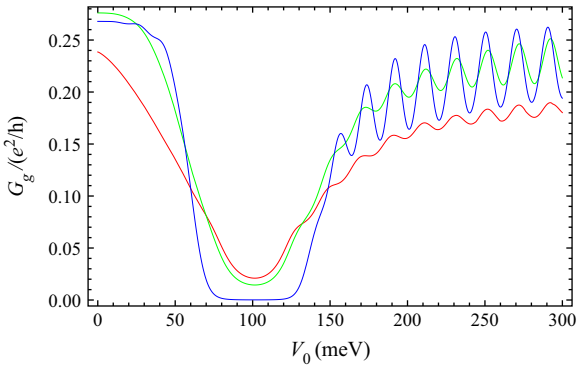

Fig. 10. Effective conductance versus the height of the barrier V_0 considering that the distribution is a Gaussian function centered around $\phi_0 = 22.5^\circ$ using different widths for the Gaussian function: $a = 0.65$ (red), $a = 0.21$ (green), $a = 0.08$ (blue). The Fermi energy is $E_F = 100$ meV and its width $D = 100$ nm. We note that as the Gaussian becomes narrower, *i.e,* as the number of inhomogeneities decreases, the conductance minimum becomes wider. (For interpretation of the references to color in this figure legend, the reader is referred to the web version of this article.)

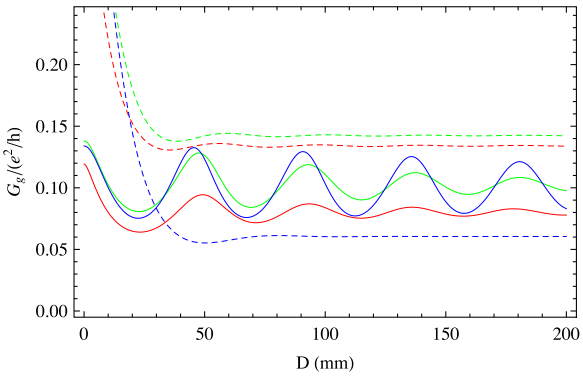

Fig. 11. Effective conductance versus the barrier width D assuming that the distribution is a Gaussian function centered around $\phi_0 = 22.5^\circ$ for $a = 0.65$ (red), $a = 0.21$ (green), $a = 0.08$ (blue) for $E_F = 50$ (line), 150 meV (dashed line) and $V_0 = 100$ meV. (For interpretation of the references to color in this figure legend, the reader is referred to the web version of this article.)

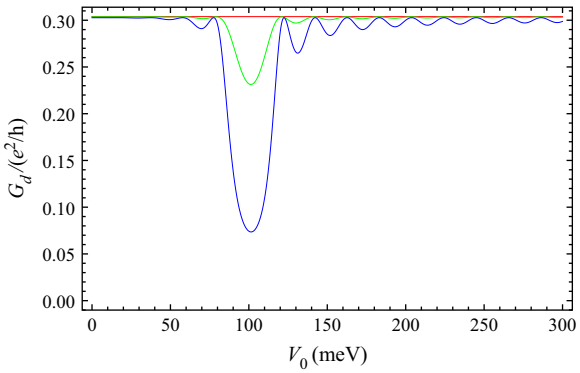

Fig. 13. Conductance versus the barrier height assuming a delta – like distribution assuming that the Fermi energy is $E_F = 100$ meV and that the width of the barrier is D = 100 nm. This calculation was performed assuming different angles of incidence $\phi_0 = 0^\circ$ (red), 2° (green) and 5° (blue). (For interpretation of the references to color in this figure legend, the reader is referred to the web version of this article.)

It is observed that the effective conductance now depends on the incidence angle, along with the rest of the parameters previously considered (Fermi energy, E_F, height of the barrier, V_0, and width of the barrier, D).

In particular, if the current flows perpendicularly to the barrier, the transmission coefficient equals 1 without dependence either on the Fermi energy or on the parameters of the barrier as a consequence of the Klein paradox [21–23]. Therefore, the conductance is proportional to the Fermi energy:

$$G_{d,0} = \frac{2}{\hbar\, v_F}|E_F|$$

For non – normal incidence, the conductance presents an effective gap between the values $\frac{V_0}{1\pm\sin\phi_0}$ of the Fermi energy, developing an effective minimum at $E_F = V_0/\cos^2\phi_0$ (as shown in Fig. 12), whose value is

$$G_{min} = \frac{2V_0}{\hbar\, v_F}\cosh^{-2}\left(\frac{DV_0\tan\phi_0}{\hbar\, v_F}\right)\cos^{-1}\phi_0$$

In this scenario, in which we assume a delta-like probability distribution function, we can see that for an angle of incidence of $\phi_0 = 22.5^\circ$ (or $\pi/8$) a wide minimum of the conductance is developed (Figs. 12 and 13). This minimum is formed when using both the Fermi energy (which can be associated with the back gate voltage of the transistor shown in Fig. 1) and the height of the barrier (the top gate voltage in our schematized model) as a driving parameter. In this case, the dependence of the conductance on the width of the barrier shows no remarkable features except for a small oscillation whose amplitude depends on the Fermi energy (see Figs. 14 and 17).

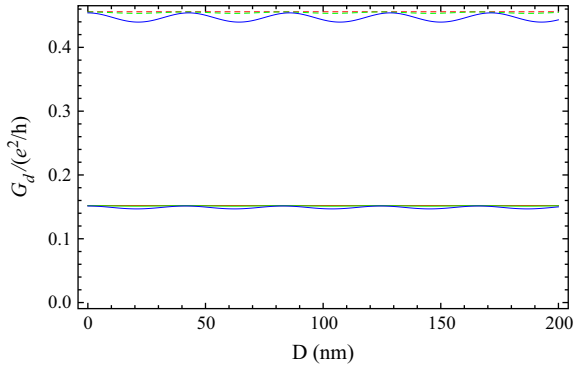

Fig. 14. Effective conductance versus the width of the barrier if a delta – like distribution probability is assumed at Fermi energies $E_F = 50$ (line), 150 meV (dashed line), and the height of the barrier potential is $V_0 = 100$ meV. We have assumed different angles of incidence: $\phi_0 = 0^\circ$ (red), 2° (green) and 5° (blue). (For interpretation of the references to color in this figure legend, the reader is referred to the web version of this article.)

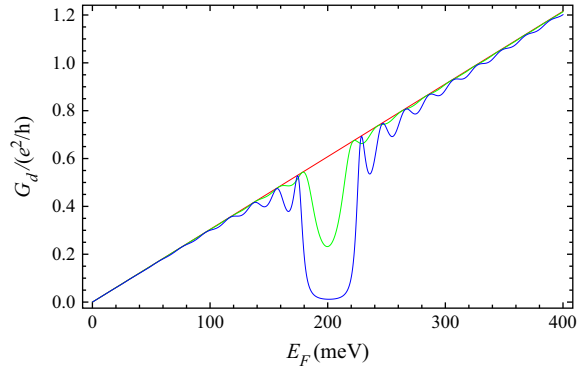

Fig. 12. Effective conductance versus Fermi energy when a delta like distribution when the height barrier is $V_0 = 200$ meV and its width $D = 100$ nm. We assume different angles of incidence: $\phi_0 = 0^\circ$ (red), 2° (green) and 5° (blue). These curves are the limit of a narrow Gaussian. (For interpretation of the references to color in this figure legend, the reader is referred to the web version of this article.)

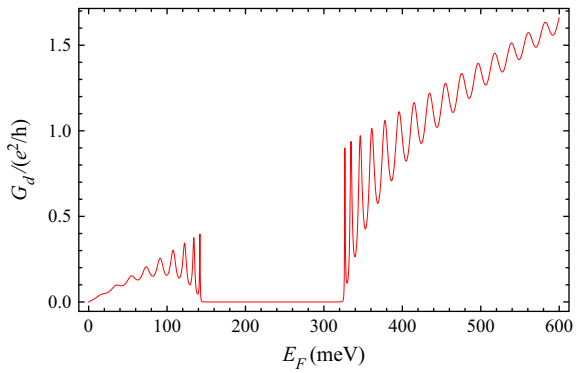

Fig. 15. Effective conductance versus the Fermi energy when a delta – like probability distribution function is assumed at an angle of incidence $\phi_0 = 22.5^\circ$ and when the potential barrier is such that $V_0 = 200$ meV and D = 100 nm.

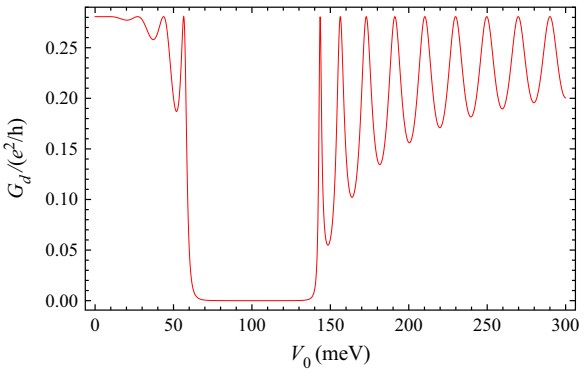

Fig. 16. Conductance versus the height of the barrier V_0 when a delta – like probability distribution function is assumed at an angle of incidence $\phi_0 = 22.5^\circ$ and the other parameters are such that $E_F = 100$ meV and $D = 100$ nm.

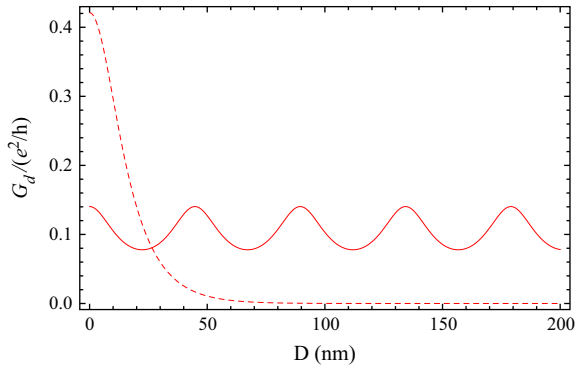

Fig. 17. Conductance versus the width of the barrier assuming a delta – like function centered around $\phi_0 = 22.5^\circ$ for $E_F = 50$ (line), 150 meV (dashed line) and $V_o = 100$ meV.

As the angle of incidence increases, the features described above tend to be greater. In particular, the effective gap that appears is wider and more pronounced, as seen in Figs. 15 and 16 where we have assumed an incidence angle $\phi_0 = 22.5^\circ$. The observed minimum of the conductance shows that in certain conditions Klein tunneling might be avoided and that the construction of an effective FET based on graphene with a noticeable on–off ratio is feasible.

4. Conclusions

In this work we have established a theoretical model in order to study transport through a square barrier potential in monolayer graphene. This model has been applied to describe the conductance between the two terminals of a graphene-based FET. The developed model considers the impact of the electrons on the potential barrier generated by the FET potential gates. To overcome the Klein effect we have considered non-perpendicular top-gates with respect to the source-drain contacts. For ballistic carriers traveling from source to drain this could induce an average angle of incidence of the carriers with the potential barrier. Of course, in a real device, disorder, impurities and any other source of scattering can produce strong deviations of this naive picture. The presence of scattering events have been modeled using different weight functions, such as gaussian probability distribution in order to effectively consider all the possible angles of incidence. We have found that for carriers reaching the barrier with non-perpendicular trajectories an effective gap is induced. Moreover this phenomenon is robust and persists when we consider the presence of disorder and inhomogeneities. Therefore, we believe that this gap might be suitable to control transport in a graphene – based field effect transistor. This phenomenon occurs for any angle of incidence ϕ_0. The position and width of the energy gap depend on both the barrier height and ϕ_0 itself. This feature might be an important step in the development of transistors based on graphene since the lack of a gap is one of the main difficulties found when attempting to modulate the current effectively via the bias.

Acknowlegements

The authors thanks José María Cerveró for useful discussions. The authors greatly acknowledge the financial support of this research by the Spanish MINECO MAT2013-46308-C2-1-R and FPU-AP2009-2619 (C.C.) and also by the Junta de Castilla y León SA226U13 and Fundación Samuel Solórzano under Project FS/21-2013.

References

[1] Castro Neto AH, Guinea F, Peres NMR, Novoselov KS, Geim AK. The electronic properties of graphene. Rev Mod Phys 2009;81:109–62.
[2] Katsnelson MI. Graphene: carbon in two dimensions. Mater Today 2007;10(1–2):20–7.
[3] Lemme MC, Echtermeyer TJ, Baus M, Kurz H. A graphene field-effect device. IEEE Electron Dev Lett 2007;28(4):282–4.
[4] Lin Y-M, Dimitrakopoulos C, Jenkins KA, Farmer DB, Chiu HY, Grill A, Avouris Ph. 100-GHz transistors from wafer-scale epitaxial graphene. Science 2010;327(5966):662.
[5] Xia F, Farmer DB, Lin Y-M, Avouris Ph. Graphene field-effect transistors with high on/off current ratio and large transport band gap at room temperature. Nano Lett 2010;10(2):715–8.
[6] Geim AK, Novoselov KS. The rise of graphene. Nat Mater 2007;6:183–91.
[7] Novoselov KS, Geim AK, Morozov SV, Jiang D, Zhang Y, Dubonos SV, et al. Electric field effect in atomically thin carbon films. Science 2004;306(5696):666–9.
[8] Geim AK. Graphene: status and prospects. Science 2009;324(5934):1530–4.
[9] Low T, Hong S, Appenzeller J, Datta S, Lundstrom MS. Conductance asymmetry of graphene p–n junction. IEEE Trans Electron Dev 2009;56(6):1292–9.
[10] Huard B, Sulpizio JA, Stander N, Todd K, Yang B, Goldhaber-Gordon D. Transport measurements across a tunable potential barrier in graphene. Phys Rev Lett 2007;98(23):236803.
[11] Gorbachev RV, Mayorov AS, Savchenko AK, Horsell DW, Guinea F. Conductance of p–n–p graphene structures with air-bridge top gates. Nanoletters 2008;8(7):1995–9.
[12] Yampolskii VA, Savelev S, Nori F. Volatge-driven quantum oscillations in graphene. New J Phys. 2008;10:053024.
[13] Young A F, Kim P. Quantum interference and Klein tunnelling in graphene heterojunctions. Nat Phys 2009;5:222–6.
[14] Begliarbekov M, Sul O, Ai N, Yang E-H, Strauf S. A periodic conductivity oscillations in quasiballistic graphene heterojunctions. Appl Phys Lett 2010;97(12):122106.
[15] Lejarreta JD, Fuentevilla CH, Diez E, Cerveró JM. An exact transmission coefficient with one and two barriers in graphene. J Phys A: Math Theor 2013;46(15):155304.
[16] Ancona MG. Electron transport in graphene from a diffusion–drift perspective. IEEE Trans Electron Dev 2010;57:681–9.
[17] Jimenez D, Moldovan O. Explicit drain-current model of graphene field-effect transistors targeting analog and radio-frequency applications. IEEE Trans Electron Dev 2011;58:4049–52.
[18] Philip Wong H-S, Akinwande D. Carbon nanotube and graphene device physics. Cambridge University Press; 2011.
[19] Datta S. Electronic transport in mesoscopic systems. Cambridge University Press; 1995.
[20] Cerveró JM, Diez E. The massless dirac equation in the refrigerator. Int J Theor Phys 2011;50(7):2134–43.
[21] Calogeracos A, Dombey N. History and physics of the Klein paradox. Contemp Phys Rev 1999;40(5):313–21.
[22] Katsnelson MI, Novoselov KS, Geim AK. Chiral tunnelling and the Klein paradox in graphene. Nat Phys 2006;2:620–5.
[23] Beenakker CWJ. Colloquium: Andreev reflection and Klein tunneling in graphene. Rev Mod Phys 2008;80(4):1337–54.
[24] Low T, Appenzeller J. Electronic transport properties of a tilted graphene p–n junction. Phys Rev B 2009;80(15):155406.